Journal of Controlled Release 311–312 (2019) 212–224

Contents lists available at ScienceDirect

Journal of Controlled Release

journal homepage: www.elsevier.com/locate/jconrel

Crosslinking: An avenue to develop stable amorphous solid dispersion with high drug loading and tailored physical stability

Anasuya Sahoo, N.S. Krishna Kumar, Raj Suryanarayanan*

Department of Pharmaceutics, College of Pharmacy, University of Minnesota, 9-177 WDH, 308 Harvard Street S.E., Minneapolis, MN 55455, United States

ARTICLE INFO

Keywords:
Amorphous solid dispersion (ASD)
High drug loading (95% w/w)
Crosslinking
Viscosity
Molecular mobility
Tailored physical stability

ABSTRACT

Influence of crosslinking (crosslinker concentration and crosslinking condition) on molecular mobility and physical stability of ketoconazole (KTZ) solid dispersions was investigated over a wide temperature range in the supercooled state. Amorphous solid dispersions (ASDs) with very high drug loading (95% w/w) were prepared by thermal crosslinking. As the crosslinker concentration increased (from 0.25–1.0% w/w), there was a progressive decrease in molecular mobility as evident from both the longer α-relaxation time, and higher viscosity values. Consequently, there was progressive enhancement in physical stability (crystallization inhibition). At 1.0% w/w crosslinker concentration, when compared with the drug alone, there was ~4 orders of magnitude increase in both viscosity and α-relaxation times. Elevating the crosslinking temperature, by increasing the crosslinking density, provided a second avenue to enhance physical stability. Hence, crosslinking density offers a simple method to enhance physical stability and control drug release. We have formulated ASDs: (i) with very high drug loading (95% w/w), and (ii) pronounced stability even when exposed to elevated temperatures and water vapor pressure. Also, during dissolution study, the degree of supersaturation in the dissolution medium generated by the crosslinked systems gradually increased and maintained the supersaturation for a longer period.

1. Introduction

One popular strategy to improve the physical stability of a non-crystalline compound is to formulate it as an amorphous solid dispersion (ASD) using a polymer [1,2]. Ideally, the polymer should exert its stabilizing effect at a low concentration. However, the risk of drug crystallization can be minimized using a high polymer concentration - an approach that is currently popular [3]. Nevertheless, in high dose drugs, this can result in an unreasonable “pill burden”. Therefore, there is a lot of interest in developing strategies to reduce the polymer concentration in ASDs.

Crosslinking the polymer provides an avenue to dramatically increase the effectiveness of the polymer as a stabilizer. Crosslinking, a process by which polymer chains are bonded to one another, leads to multidimensional extension of polymeric chains resulting in a network structure. Depending upon the nature of the polymer, crosslinking can be accomplished chemically [4–6], thermally [7], physically [8] or by γ irradiation [9]. Chemical crosslinking refers to intermolecular or intramolecular joining of two or more molecules by a covalent bond. The reagents that are used for the purpose are referred to as ‘crosslinking reagents’ or ‘crosslinkers’ [10]. Crosslinking leads to an increase in the mechanical strength, viscosity and the glass transition temperature (T_g) [11–13]. However, the process can result in undesirable properties – the insoluble nature of crosslinked systems are potentially serious limitations [12]. Hydrogels are one of the upcoming class of crosslinked hydrophilic polymer structures that can imbibe a large amount of water or biological fluids [13–17] but will not dissolve. Because of their biocompatibility, they have numerous biomedical applications – for example, as matrices for protein delivery systems and as tissue engineering scaffolds.

In the polymer industry, the decrease in molecular mobility brought about by crosslinking has been used as an avenue to improve thermal as well as physical stability of the polymer. The molecular mobility can be measured by various techniques including modulated DSC [18], high-resolution solid-state ^{13}C NMR [19], dynamic mechanical analysis (DMA) [20] and dielectric spectroscopy (DES) [21]. DES, a widely used technique to characterize different mobility modes in polymers, enables the direct determination of relaxation times [21–26]. Crosslinking affects both the primary and secondary relaxation of polymer systems [22]. The degree of crosslinking influenced the relaxation time, fragility, dielectric strength, and the distribution of relaxation times [23].

The potential for enhancing the delivery of poorly soluble drugs by

* Corresponding author.
E-mail address: surya001@umn.edu (R. Suryanarayanan).

https://doi.org/10.1016/j.jconrel.2019.09.007
Received 16 July 2019; Received in revised form 4 September 2019; Accepted 5 September 2019
Available online 06 September 2019
0168-3659/

incorporating in a crosslinked hydrogel was explored by Zahedi and Lee [27]. When indomethacin was incorporated in crosslinked poly (2-hydroxyethyl methacrylate), amorphous ➔ crystalline transition of the drug was not observed up to a drug loading of 30%. In addition, during dissolution, the absence of a decline in drug concentration indicated that drug crystallization was prevented [28]. However, the study did not focus on developing a systematic understanding of the mechanism by which crosslinking induced stabilization.

Again, the effect of crosslinking on the molecular mobility and physical stability of ASDs has not been comprehensively investigated. In order to effectively use this approach in the design and preparation of ASDs, it is necessary to understand the mechanism governing the physical stability brought about by crosslinking. We hypothesize that crosslinking, by increasing, the viscosity of the ASD, will decrease the mobility and consequently the crystallization propensity of the drug.

The model drug ketoconazole (KTZ) is known to have a high propensity to crystallize [29]. Poly (acrylic acid) (PAA) and poly (vinyl alcohol) (PVA) were chosen as the model polymer and crosslinker, respectively. Zahedi and Lee [27], used a chemical crosslinking process to fabricate the amorphous solid dispersion. However, we have used thermal crosslinking, a "clean" process with no requirement of a chemical crosslinker or an initiator for the crosslinking reaction. Moreover, we were able to prepare ASDs with exceptionally high drug loading (up to 95% w/w). Unlike chemical crosslinking, in our approach, the drug loading is not limited by the crosslinking density. This study had two objectives. (i) Investigate the influence of crosslinking of the polymer on the molecular mobility (measured as α-relaxation time) of ASDs with high drug loading (95% drug). (ii) Evaluate the effect of crosslinker concentration and crosslinking conditions (temperature and time of crosslinking) on the molecular mobility and crystallization propensity of KTZ.

We believe that we are the first to: (i) study the molecular mobility of the crosslinked amorphous solid dispersions using DES and (ii) develop a fundamental understanding of the effect of crosslinking on molecular mobility of amorphous solid dispersions. We have also successfully demonstrated that, the degree of crosslinking, i.e. crosslinking density, provides an avenue to modulate the physical stability of ASDs. This can be accomplished by tuning the crosslinker concentration and the reaction temperature.

2. Experimental section

2.1. Materials

Selection of model compounds (Fig. 1a) was based on several attributes. Ketoconazole, an imidazole antifungal agent, possess some antibacterial activity. The model drug KTZ is a weak base with two pKa values: 6.5 and 2.94 [30,31]. KTZ can be readily rendered amorphous by melt quenching, and it is chemically stable at least up to 10 °C above its melting point [32,33]. There are no reported polymorphic forms of anhydrous KTZ [34]. The molecular structure of PAA, PVA and drug (KTZ) are shown in Fig. 1a. Ketoconazole (purity > 98%) was a gift from Laborate Pharmaceuticals (Haryana, India), PAA (Mw 1500) and PVA (Mw 6000) were purchased from Sigma Aldrich and used without any further purification. The polymer and the crosslinker were dried at 110 °C for 1 h and stored in a desiccator containing anhydrous calcium sulfate until used.

2.2. Preparation of amorphous KTZ

Crystalline KTZ was heated to 160 °C, held for 1 min, and cooled rapidly in liquid nitrogen. The quenched materials were then gently ground using a mortar and pestle to obtain a free-flowing powder and stored at −20 °C in a desiccator containing anhydrous calcium sulfate until used. All the sample preparation and subsequent handling were done in a glovebox (RH < 5%) at room temperature.

2.3. Preparation of crosslinked amorphous solid dispersions with KTZ

Table 1 lists the crosslinking conditions and the compositions of the different ASD systems. PAA, PVA and KTZ were dissolved in dimethyl formamide (DMF) by heating at 80 °C for 5 min. The solvent was removed using a rotary evaporator (IKA-HB10 digital system rotary evaporator, Werke. GmbH and Co., Staufen, Germany) at 70 °C under reduced pressure (25 mm of Hg). The powder was then dried at 70 °C under reduced pressure for 45 min. ASDs were further dried for 12 h in a vacuum desiccator at RT. Then the system was crosslinked at 135 °C for 2 h to induce esterification reaction between the carboxylic acid group of PAA and the hydroxyl group of PVA to produce the crosslinked ASDs (Fig. 1b). Crosslinked ASDs with 90% (w/w) drug loading were subjected to detailed characterization. In addition, dispersions with 95% (w/w) drug loading were also prepared. However, crystallization was observed during crosslinking, when the reaction was carried out at 135 °C. Hence, a modified method was used to prevent drug crystallization during crosslinking. After the solvent evaporation, the samples were crosslinked, either at the melting temperature of the drug (150 °C) or at 170 °C for 15 min. For comparison purposes, cross-linked systems with 90% drug loading were also prepared. Numerous batches of each composition were prepared (≥6). All the samples were stored at −20 °C until further use. Sample handling was done in a glove box (RH < 5%) at RT.

2.4. Volumetric swelling study

Gel disks, ~1.5 cm diameter and 0.54 mm thick, were immersed in deionized water (DI) and allowed to achieve equilibrium swelling at room temperature. The disks were patted dry carefully to remove only the surface water and weighed. The disks were then dried in an oven and the % swelling was calculated using Eq. (1):

$$\text{Swelling}\% = \frac{W_t}{W_0} \times 100 \quad (1)$$

W_t = weight of swollen disk at time t and W_0 = weight of dry disk.

2.5. Differential scanning calorimetry (DSC)

A differential scanning calorimeter (TA instruments Q2000, Delaware, USA) equipped with a refrigerated cooling unit was used. The instrument was calibrated with indium, hermetically sealed in a T zero pan. The sample powder was accurately weighed in aluminum pans and sealed hermetically. The weighing was carried out in a glovebox. All the measurements were done under dry nitrogen purge (50 ml/min) at a heating rate of 10 °C/min. Data were analyzed using Universal Analysis software (TA Instruments, New Castle, DE). Glass transition temperature (T_g) was the midpoint of the transition and the crystallization peak temperature (T_c) was the peak temperature of the enthalpy of crystallization peak.

2.6. X-ray diffractometry

A powder X-ray diffractometer (D8 ADVANCE; Bruker AXS, Madison, WI) equipped with a variable temperature stage (TTK 450; Anton Paar, Graz-Straβgang) and a one-dimensional silicon detector (LynxEye, Bruker AXS) was used. Using Cu Kα radiation (1.54 Å; 40 kV × 40 mA) data were collected, over the angular range of 5–35° 2θ, with a step size of 0.05° and a dwell time of 0.5 s.

2.7. Variable temperature X-ray powder diffractometry (VTXRD)

The samples were subjected to XRD using a controlled temperature program. The diffraction data were collected over the angular range of 5–35° 2θ with a step size of 0.05° 2θ and 0.5 s dwell time. The measurements were performed in 10 °C increments from 30 °C up to 170 °C.

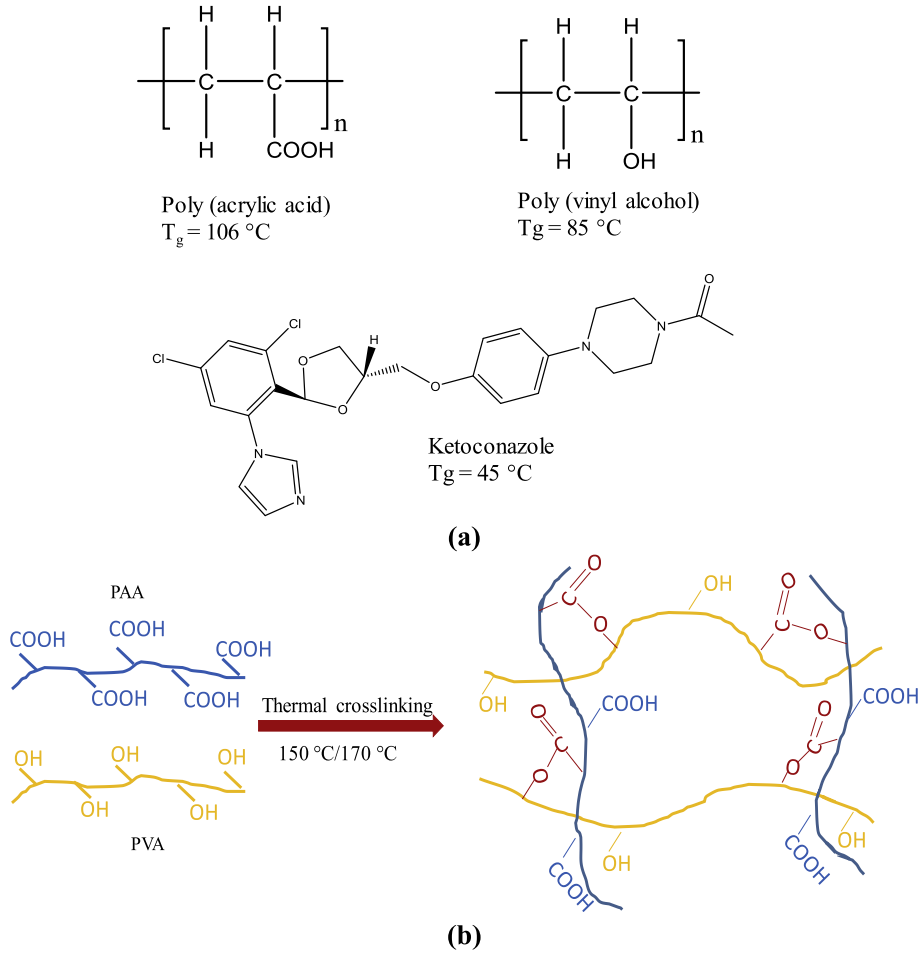

Fig. 1. a) Structures of poly acrylic acid (PAA), polyvinyl alcohol (PVA), and ketoconazole (KTZ). b) Proposed structure following the crosslinking of PAA with PVA (the esterification reaction leading to the crosslinked system) [35].

Table 1
Compositions of the ASD systems and the crosslinking conditions.

Sample ID	Crosslinking conditions		PAA (% w/w)	PVA (% w/w)	KTZ (% w/w)
	Temp (°C)	Time (min)			
A1	135	120	9.75	0.25	90
A2	135	120	9.50	0.50	90
A3	135	120	9.25	0.75	90
A4	135	120	9.00	1.00	90
A5	135	120	8.00	2.00	90
A6	135	120	7.00	3.00	90
A7	135	120	6.00	4.00	90
A8	135	120	5.00	5.00	90
B1	150	15	9.75	0.25	90
B2	150	15	9.50	0.50	90
B3	150	15	9.25	0.75	90
C3	170	15	9.25	0.75	90
B4	150	15	9.00	1.00	90
B3H	150	15	9.25	0.75	95
C3H	170	15	9.25	0.75	95
D1	NC [a]	NC	10.00	NA	90
D2	NC	NC	5.00	NA	95

NC [a]- no crosslinking.
A - crosslinked at 135 °C/120 min.
B - crosslinked at 150 °C/15 min.
C - crosslinked at 170 °C/15 min.
H - 95% drug loading.
D1 - 90% drug, 10% PAA and no crosslinker.
D2 - 95% drug, 5% PAA and no crosslinker.

The heating rate was 12 °C/min, and the sample was maintained under isothermal conditions during each XRD experiment (~5 min).

2.8. Water sorption analysis

The water sorption profiles of the crosslinked ASDs were obtained using an automated vapor sorption analyzer (Q5000, TA instruments). Approximately 15 mg of powder was placed in a quartz sample pan, and equilibrated at 0% RH (25 °C) for 6 h under a nitrogen flow rate of 200 ml/min. The RH was then increased to 90% and held for up to 7000 min. The first time point when a weight loss was observed (the weight change as a function of time (dm/dt) reaches a negative value) was taken as the crystallization onset time. The sample was removed, crimped hermetically in an aluminum pan and subjected to DSC.

2.9. Dielectric spectroscopy (DES)

A dielectric spectrometer (Novocontrol Alpha-AK high performance frequency analyzer, Novocontrol Technologies, Germany) equipped with a temperature controller (Novocool Cryosystem) was used to perform isothermal dielectric measurements over the frequency range of 10^{-2}–10^{7} Hz. The experimental temperature range, −100 to 200 °C, covers both the glassy and supercooled liquid regions. The amorphous sample, in powder form, was placed between two gold-plated copper electrodes (20 mm diameter), separated by a polytetrafluoroethylene (PTFE) spacer (1 mm thickness, 59.69 mm^2 area). The spacer was used to confine the sample between the electrodes.

2.10. Viscosity

A rheometer equipped with a forced convection oven (ARES G2, TA Instruments) was used. The measurements were done in parallel plate configuration (8 mm diameter) in oscillatory mode with continuous nitrogen purge. Approximately 300 mg of sample was placed on the bottom plate, and then the gap was closed by bringing down the upper plate until a normal force was recorded. The samples were heated to 155 °C, held for a minute and then cooled to 110 °C. At first, a dynamic strain sweep was recorded at a fixed frequency of 1 rad/s in the strain range of 0.1–100% and the linear viscoelastic region (LVR) was confirmed. The dynamic frequency sweep test was performed within the LVR, at a fixed strain (10%) over the frequency range of 0.1–100 rad/s, and the complex viscosity, the loss modulus (G″) and the storage modulus (G′) values were recorded. Only the viscosity results are discussed. For plotting the viscosity as a function of temperature, the complex viscosity (η) at a frequency of 1 rad/s was used.

2.11. Powder dissolution

A USP type II (Varian 705 DS, Agilent Technologies, Santa Clara, CA) dissolution apparatus was used and the paddle speed was 100 rpm. The powder (650 mg; KTZ equivalent) was dispersed in 500 ml of the dissolution medium (phosphate buffer solution (pH 6.8) containing 0.15% sodium lauryl sulfate) maintained at 37 °C. Aliquots were taken at predetermined time points, filtered (0.45 μm PTFE syringe filter) and the absorbance measured at 291 nm using a UV-VIS spectrophotometer (Cary 100 Bio UV/Vis, Agilent Technologies). The dissolution volume was kept constant throughout the experiment. The area under the concentration – time curves (AUC) were determined by noncompartmental analysis by the trapezoidal rule integration to the last time point ($AUC_{0\rightarrow t}$) using commercial software (Phoenix WinNonlin version 6.4, Certara USA, Inc., Princeton, NJ). The extent of dissolution enhancement was quantified from the AUC ratio ([$AUC_{(0\rightarrow t)}$, sample]/[$AUC_{(0\rightarrow t)}$, crystalline KTZ]).

3. Results & discussion

The structure of the model drug (KTZ), polymer (PAA) and crosslinker (PVA) are given in Fig. 1a. ASDs were prepared by solvent evaporation method with 90% and 95% w/w drug loading. Then the system was crosslinked to induce the esterification reaction between carboxylic acid group of PAA and hydroxyl group of PVA to produce the crosslinked ASDs (Fig. 1b). The detailed procedure for ASD preparation and their subsequent crosslinking process are given in the experimental section. Table 1 lists the compositions of the different ASD systems and the crosslinking conditions. In all cases, > 99.5% of KTZ was retained, reflecting the exceptional thermal stability of the drug under the crosslinking conditions (Table S1; Supplementary Information).

3.1. Volumetric swelling study to determine the crosslinking density

To understand the effect of crosslinker concentration on crosslinking density, volumetric swelling study was carried out. The equilibrium-swelling ratio (qm) is achieved when the swelling ratio (q), no longer changes with time. The crosslinker concentration and crosslinking density will influence the qm value and is expected to increase with decreasing crosslinking density (crosslinker concentration) [36,37]. This is indeed the behavior observed from the swelling experiments and is consistent with earlier studies [36,37]. The qm of the crosslinked systems are shown in Fig. 2a.

With an increase in the crosslinker concentration, for example, from 0.25% (B1) to 1% (w/w) (B4), the equilibrium swelling value (qm) was lower and was achieved earlier. For B4, qm was achieved in ~1000 min whereas, for B1, it was ~1500 min. In addition, the qm for B4 and B1 are ~150% and ~250% respectively (Fig. 2a). The slope (m) value, an indicator of the swelling kinetics, was strongly dependent on the crosslinker concentration. B1 has a higher slope (m = 2.8) than B4 (m = 1.3). The slope of the initial swelling is an indicator of the kinetics of swelling, which means the rate of swelling of B1 is high compared to that of B4. With an increase in the crosslinker content, the slope value decreased indicating that the rate of swelling decreases with increase in crosslinker concentration. The swelling rate is an indirect method to measure the crosslinking density – higher the swelling rate, lower is the crosslinking density [36,37]. So, it can be concluded that with increase in crosslinker concentration the crosslinking density increases.

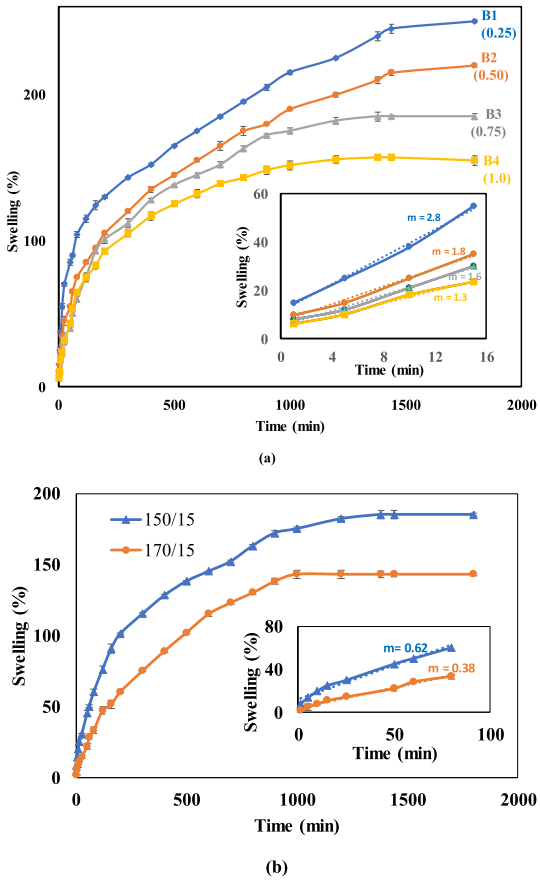

Fig. 2. a) Effect of crosslinker concentration on swelling kinetics and equilibrium swelling. All the ASDs were crosslinked at 150 °C for 15 min. Inset: Effect of crosslinker concentration on initial swelling rate. The swelling rate m (slope of the line, expressed as %/min), is given above each curve. b) Effect of crosslinking temperature on swelling kinetics and equilibrium swelling. The crosslinker concentration was 0.75% w/w and crosslinked, either at 150 °C (B3; triangle) or at 170 °C (C3; circle) for 15 min. Inset: Effect of crosslinking temperature on initial swelling rate. Error bars represent SD. In some cases, they are smaller than the size of the symbol.

The effect of crosslinking temperature on the degree of crosslinking is evident from the results in Fig. 2b. At a fixed crosslinker concentration of 0.75% w/w, the crosslinking was conducted either at 150 °C or at 170 °C. The higher crosslinking temperature (170 °C) showed a lower qm (~140%) and - slower attainment of equilibrium swelling (Fig. 2b). The same behavior was observed in the initial swelling rate (Fig. 2b; inset).

3.2. Thermal analysis

The melt-quenched KTZ as well as the KTZ ASDs were observed to be X-ray amorphous (data is not shown). The DSC heating curve of amorphous KTZ revealed a baseline shift at 44.3 °C attributable to glass transition (T_g) followed by onset of crystallization at 97.2 °C,

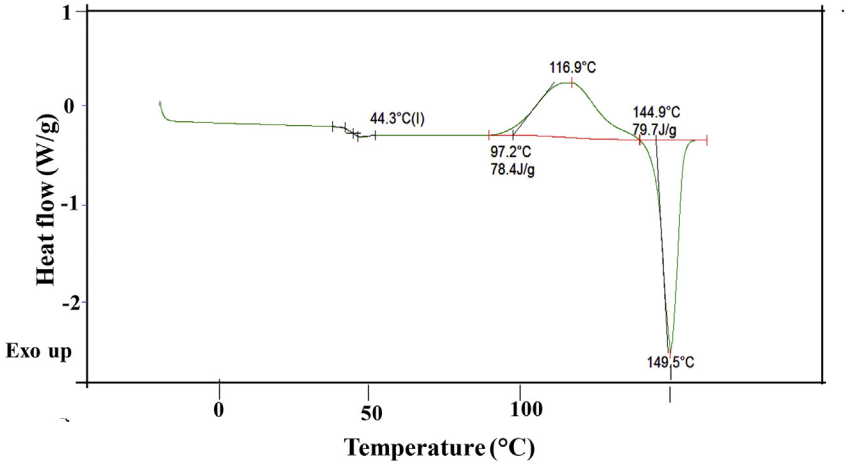

(a)

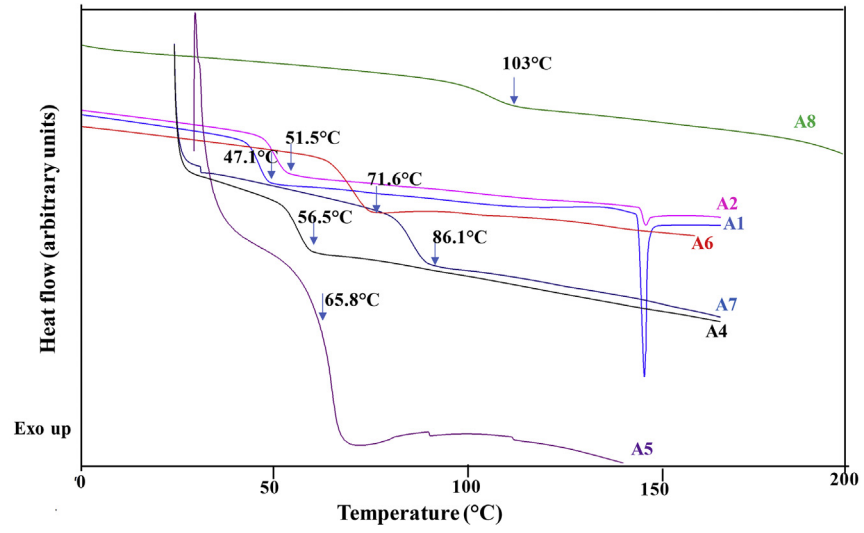

(b)

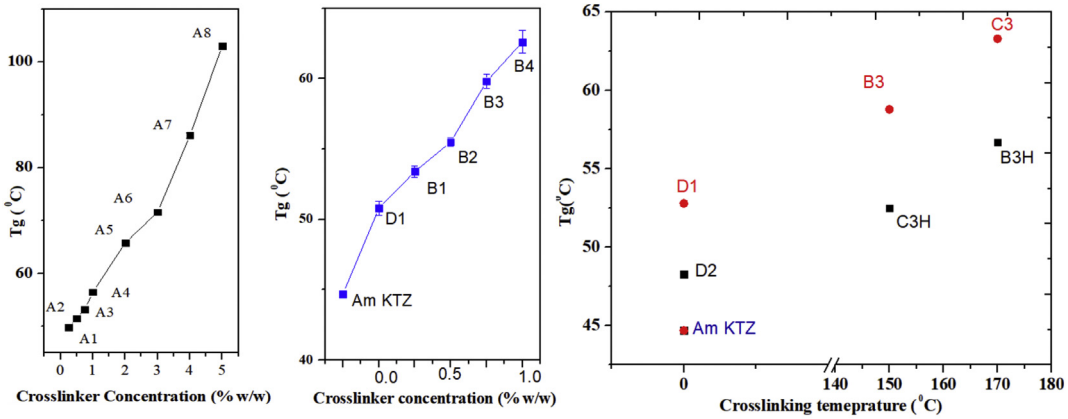

(c) (d) (e)

Fig. 3. a) DSC heating curve of amorphous KTZ (Am KTZ). b) DSC heating curves of ASDs crosslinked at 135 °C for 2 h. The drug loading was 90% w/w (compositions are in Table 1). c) Effect of crosslinker concentration on the T_g of the ASDs (90% drug loading; crosslinked at 135 °C for 120 min). d) crosslinked at 150 °C for 15 min. e) Effect of crosslinking condition on the T_g of the ASDs. The compositions are given in Table 1. Error bars represent SD. In some cases, they are smaller than the size of the symbol.

Table 2
Thermal properties (from DSC) and temperature of crystallization (first evidence in variable temperature XRD) of the crosslinked ASDs.

Sample ID	Drug loading (%)	Crosslinking condition		T_g (°C)	T_C (°C)	ΔH (J/g)	T_m (°C)	ΔH (J/g)	1st evidence of crystallization (°C)
		Temp (°C)	Time (min)						
KTZ[a]	100	NA	NA	44.7 ± 0.8[b]	116.9 ± 1.2	78.4 ± 0.8	146 ± 1.3	77.9 ± 3.9	85.0
A1	90	135	120	47.3 ± 0.4	136.0 ± 0.5	2.57 ± 3.2	147.0 ± 0.3	3.53 ± 3.9	110.0
A2	90	135	120	51.5 ± 0.5	144.0 ± 0.5	0.33 ± 0.1	147.0 ± 0.2	0.32 ± 0.1	115.0
A3	90	135	120	53.2 ± 0.5	NC[c]				145.0
A4	90	135	120	56.5 ± 0.2	NC				NC
A5	90	135	120	65.8 ± 0.1	NC				NC
A6	90	135	120	71.6 ± 0.3	NC				NC
A7	90	135	120	86.1 ± 0.5	NC				NC
A8	90	135	120	103.0 ± 0.2	NC				NC
B1	90	150	15	53.4 ± 0.4	NC				NC
B2	90	150	15	55.5 ± 0.1	NC				NC
B3	90	150	15	59.8 ± 0.5	NC				NC
C3	90	170	15	63.3 ± 0.2	NC				NC
B4	90	150	15	62.6 ± 0.8	NC				NC
B3H	95	150	15	52.5 ± 0.6	NC		149.0 ± 1.3	0.16 ± 0.1	135.0
C3H	95	170	15	56.7 ± 1.3	NC				NC
D1	90	NA	NA	52.8 ± 0.8	NC				NC
D2	95	NA	NA	50.2 ± 0.6	117.2 ± 0.8	0.24 ± 0.5	147.0 ± 0.5	0.4 ± 0.1	115.0

D1, D2: contains only drug and polymer (PAA) and no crosslinker (PVA).
[a] Amorphous KTZ (no polymer).
[b] Mean ± SD; n ≥ 3.
[c] NC, no crystallization.

crystallization at 116.9 °C (peak temperature T_c) and finally melting at 149.5 °C (Fig. 3a). The observed T_g value and the crystallization and melting temperatures were in excellent agreement with literature reports [38,39].

The dispersions crosslinked at 135 °C for 2 h, irrespective of the composition, revealed a single T_g (Fig. 3b). The T_g of A1 was close to that of D1 (Fig. 3c, Table 2). This is not surprising in light of the low crosslinker concentration. With progressive increase in crosslinker concentration, the T_g shifted to higher temperatures (Fig. 3 c, d and Table 2). This T_g rise is attributed to the increase in the number of crosslinks, thereby restricting the molecular motion of the polymer chains and reducing the free volume [40].

At low crosslinker concentrations, (A1 and A2: Table 1), there was evidence of KTZ crystallization when the sample was heated above T_g. The crystallization occurred over a wide temperature range (shallow exotherm) and was followed by a KTZ melting endotherm. At a crosslinker concentration of 0.25% w/w, there was pronounced sample to sample variation in the enthalpy of crystallization (2.57 ± 3.2 J/g; $n = 3$) and consequently in the enthalpy of fusion (3.53 ± 3.9 J/g). When the crosslinker concentration was increased, there was a pronounced inhibition in crystallization (crystallization enthalpy: 0.33 ± 0.04 J/g). At higher crosslinker concentrations (PVA concentration ≥ 0.75% w/w), KTZ crystallization was completely inhibited. Consequently, the melting peak was also not observed (Fig. 3b). However, under this reaction condition (135 °C for 2 h), there is a potential for drug crystallization when the crosslinker concentration is low. In an effort to minimize the risk of drug crystallization, we increased the crosslinking temperature to 150 °C. Since this is above the melting point of the drug (147 °C), there is no risk of nucleation/crystallization during the crosslinking reaction. Moreover, from our preliminary experiments, we determined that the reaction time could be decreased to 15 min at this crosslinking temperature.

At all crosslinker concentrations, the increase in the crosslinking temperature from 135 °C to 150 °C, caused a shift in the T_g to a higher temperature. As expected, there was a progressive increase in T_g as a function of crosslinker concentration (Fig. 3c and d; DSC curves are provided in Fig. S1; Supplementary Information). Even at the lowest crosslinker concentration, there was no evidence of KTZ crystallization when heated up to its melting temperature (Fig. S1 in Supplementary Information; Table 2). Therefore, the crosslinking density was sufficient to inhibit drug crystallization.

The effectiveness of the crosslinking condition (150 °C/15 min) was next evaluated at a higher drug loading of 95% w/w and at a fixed crosslinker concentration of 0.75% w/w. A weak melting endotherm (enthalpy: 0.16 ± 0.10 J/g) was discernible at 149 °C, indicating drug crystallization during the DSC run (Fig. S2, B3H in Supplementary Information; data in Table 2). However, when the crosslinking temperature was increased to 170 °C (for 15 min), the melting endotherm was no longer observed (Fig. S2b; data in Table 2). Thus, even when the drug loading is very high, crystallization inhibition can be accomplished by elevating the crosslinking temperature.

At the high crosslinking temperature of 150 °C, as pointed out earlier, both phase separation and crystallization of drug may have been inhibited by the presence of thermal crosslinks. The T_g increased by about 9 °C for an increase in the PVA concentration, from 0.25 to 1.0% w/w (Fig. 3d). The effect of the crosslinking temperature on T_g is evident from Fig. 3e. It clearly showed an increase in the T_g of both the ASDs (C3 & C3H). This is attributed to the increase in crosslinking at high crosslinking temperature that restricts the molecular mobility of the polymer chains and reduces the free volume of the system and leads to the increase in T_g [40].

3.3. Influence of crosslinking density on the molecular mobility

Dielectric spectroscopy provides an avenue to measure the molecular mobility of the glass-forming systems. Molecular mobility of pharmaceutical interest may be broadly classified into global mobility (characterized by α-relaxation) and local mobility (β-relaxation) [41].

The complex dielectric function ε*(ω), as a function of frequency (ω).

$$\varepsilon^*(\omega) = \varepsilon'(\omega) - i\varepsilon''(\omega), \quad (2)$$

consists of the real part [ε′(ω)], describing the stored energy and the imaginary part [ε″(ω)] representing the dissipated energy over a frequency range.

Conventionally, the relaxation time is obtained from a plot of the dielectric loss as a function of frequency. In our systems, the analyses were complicated by (i) the high conductivity contribution to the dielectric loss (ε″(ω)) and (ii) the effect of electrode polarization on the real part of permittivity (ε′(ω)). Therefore, the data were analyzed

using Eq. (3).

$$\varepsilon^*(\omega) = \varepsilon_\infty + \frac{\Delta\varepsilon}{(1 + (i\omega\tau_{HN})^\alpha)^\gamma} + \frac{\sigma_0}{i\omega\varepsilon_0} + A\omega^{-n} \quad (3)$$

where ε_0 is the free space dielectric constant, ε_∞ is the high frequency dielectric constant, $\sigma_0/i(\omega\varepsilon_0)$ is the dielectric loss contribution due to dc conductivity (σ_0).

The electrode polarization contribution to the real part of the dielectric constant can be described by a power law dependence $A\omega^{-n}$ (first order approximation), where A is the strength of the electrode polarization and n is the exponent. The α-relaxation process is modelled with the Havriliak-Negami (HN) function (2nd term of Eq. (3)), where $\Delta\varepsilon$ is the dielectric strength of the α-relaxation process, τ_{HN} is the HN relaxation time and, α and γ are the shape parameters which respectively determine the symmetric and asymmetric broadening of dielectric loss peak. The dielectric relaxation time (τ) is determined from the peak maximum frequency of dielectric loss peak. The τ value is obtained from the HN parameters using Eq. (4) [42].

$$\tau = \tau_{HN}\left[\sin\left(\frac{\alpha\pi}{2 + 2\gamma}\right)\right]^{-1/\alpha}\left[\sin\left(\frac{\alpha\gamma\pi}{2 + 2\gamma}\right)\right]^{1/\alpha} \quad (4)$$

Dielectric plots of ε′ and ε″ as a function of frequency, for a few representative crosslinked systems, are shown in Fig. S3 (Supplementary Information). It is evident from the plots that the modified HN equation (Eq. (3)) effectively accounts for the contributions of polarization and conductivity. Therefore, the α- relaxation time could be unambiguously determined, and the results have been tabulated in Table S2 (Supplementary Information). As expected, at a given crosslinker concentration, the relaxation times decreased as a function of temperature (Fig. 4a and b). An increase in crosslinker concentration caused a progressive decrease in relaxation time (Fig. S4 and Table S2; Supplementary Information).

The temperature dependence of τ followed the Vogel-Fulcher-Tammann (VFT) relationship.

$$\tau = \tau_\infty \exp\left(\frac{DT_0}{T - T_0}\right) \quad (5)$$

where τ_∞ is the relaxation time of at "infinite" temperature, D is the strength parameter and T_0 is the zero-mobility temperature (Fig. 4). The mere addition (weight fraction of 0.1) of polymer (D1 in Table 1), caused a pronounced (~2 orders of magnitude) decrease in mobility. The results were in excellent agreement with previous findings [43].

The addition of crosslinker, at a concentration of 0.25% w/w, had no appreciable effect on mobility. This was in agreement with our DSC results, where the thermal properties (T_g, T_c and crystallization enthalpy) were the same for the control (D1) and the crosslinked system A1 (Fig. 3). However, higher crosslinker concentrations had a pronounced effect on mobility. A change in crosslinker concentration from 0.25 to 1.0% w/w, resulted in ~2 orders of magnitude increase in relaxation time. This becomes readily evident when the relaxation times are compared at a fixed temperature, say at 100 °C (Fig. S4; Supplementary Information). With increase in crosslinker concentration, the width of dielectric loss peak decreases reflecting a narrowing in the distribution of relaxation times (Fig. S4; Supplementary Information). The Kohlrausch-Williams-Watts (KWW) stretched exponential relaxation function (ϕ(t)) can be used to obtain the distribution of relaxation times [44].

$$\phi(t) = \exp[-(t/\tau_{KWW})^{\beta_{KWW}}] \quad (6)$$

In Eq. (6), ϕ(t) is the relaxation function in time-domain, τ_{KWW} is the characteristic KWW relaxation time and β_{KWW} is the exponent and its value can be $0 < \beta_{KWW} \leq 1$. The β_{KWW} values were obtained from the HN parameters α and γ using the empirical equation [45].

$$\beta_{KWW}^{1.23} = \alpha\,\gamma \quad (7)$$

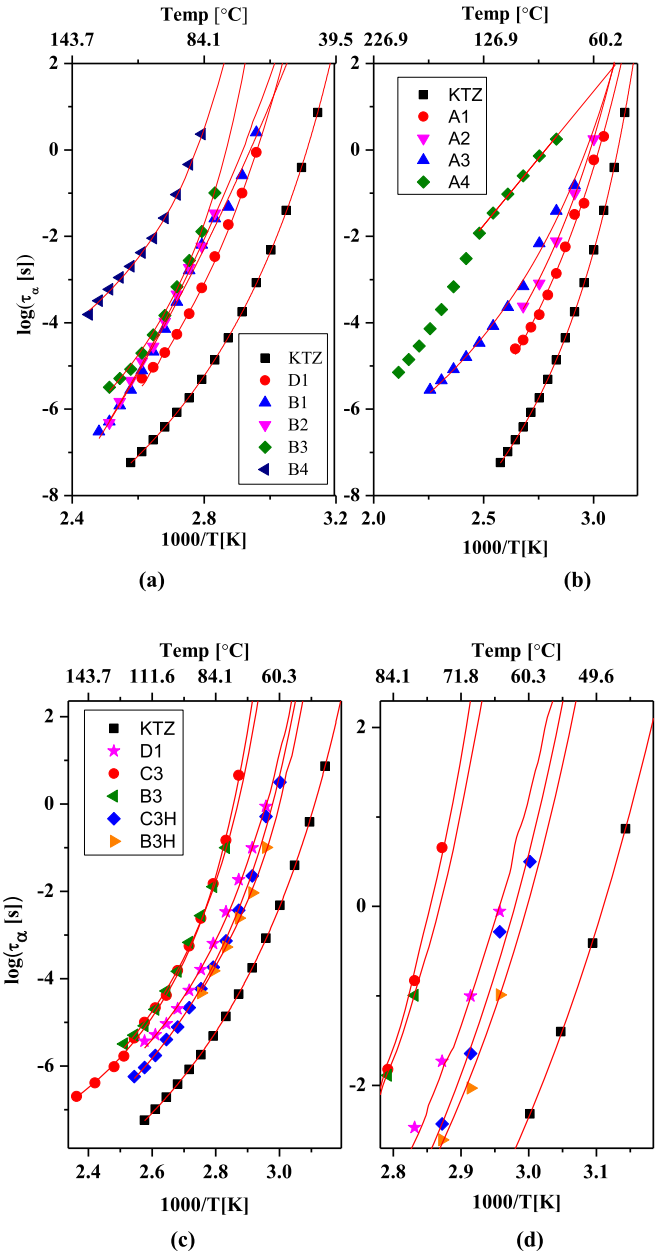

Fig. 4. Temperature dependence of α-relaxation time in ASDs with 90% w/w drug loading and crosslinker concentration ranging from 0.25 to 1.0% w/w. The systems were crosslinked at a) 150 °C for 15 min and b) 135 °C for 120 min. c) Temperature dependence of α-relaxation times in ASDs (drug loading 90 or 95% w/w) with a fixed crosslinker concentration (0.75% w/w) and crosslinked either at 150 °C or at 170 °C, and d) is the enlarged view of panel (c) over a narrow temperature range. The compositions are given in Table 1. The y-axis is the logarithm of relaxation time and the error bars are smaller than the symbol size.

Decreased value of β_{KWW} may be an indication of increased heterogeneity [46]. With increase in crosslinker concentration, a systematic narrowing in relaxation time distribution (increase in the value of β_{KWW}) was observed, an indication of decrease in heterogeneity (Table S2; Supplementary Information). The β_{KWW} parameter may provide a measure of the physical stability of amorphous systems [47]. The glass formers with broader distribution of structural relaxation times (low β_{KWW} value) may be more susceptible to nucleation resulting in reduced physical stability [48]. The β_{KWW} values, as well as the resistance to crystallization (discussed later), progressively increased as a

function of the crosslinker concentration.

As pointed out earlier, the crosslinking temperature and duration provided another avenue to modulate the number of crosslinking points in the network (crosslinking density). At a fixed crosslinker concentration of 0.75% w/w, crosslinking was carried out at 135, 150 and 170 °C. An increase in crosslinking temperature caused a decrease in molecular mobility reflected by an increase in the relaxation time. As evident from Table S2 (Supplementary Information), the molecular mobility at lower temperatures (< 80 °C) can be rank ordered as: A3 > B3 > C3 (compositions are given in Table 1). This suggests an increase in crosslinking density as a function of reaction temperature.

3.4. Variable temperature X-ray diffractometry of ASDs

The physical stability of the systems was also evaluated by obtaining the X-ray diffraction patterns while subjecting them to a controlled temperature program. The crystallization behavior of KTZ was first evaluated. On heating amorphous KTZ, crystallization was clearly evident at 85 °C (Fig. S5; Supplementary Information). DSC had revealed crystallization onset at a slightly higher temperature of ~97 °C. We had earlier pointed out that, at low crosslinker concentrations, reaction at 135 °C (for 2 h) has the potential to cause drug crystallization. Therefore, our current studies were restricted to the higher crosslinking temperatures of 150 and 170 °C. Powder X-ray diffraction patterns of the dispersions crosslinked at 150 °C (B1 to B8) revealed their amorphous nature confirming that there was no crystallization *during* crosslinking (Fig. 5a).

When the systems with 90% w/w drug loading (B1-B4; crosslinked at 150 °C for 15 min) were subjected to variable temperature XRD (VTXRD), there was no evidence of crystallization when heated up to 170 °C (Fig. S6; Supplementary Information). Interestingly, even in the absence of crosslinker (10% PAA with no crosslinker; D1 in Table 1), crystallization was not observed when heated up to 170 °C. Thus, the stabilizing effect of crosslinking, if any, could not be discerned from VTXRD. Therefore, the drug loading was increased to 95% w/w. In the absence of crosslinking, crystallization was first evident at 105 °C (D2, Fig. 5b). However, crosslinking (B3H) elevated the crystallization temperature to 135 °C (Fig. 5c). Thus, when crosslinked, the system was able to resist crystallization to a temperature $\gg T_g$ [$(T - T_g) > 80$ °C].

Since crosslinking was carried out above the melting temperature of the drug, the positions of the randomly distributed drug molecules are "fixed" by the crosslinks thereby retarding the crystallization propensity of the drug. The consequent reduction in mobility, as evident from DES (Fig. 4), had a pronounced inhibitory effect on drug crystallization. This is evident from the DSC results, wherein only a very weak endotherm attributable to KTZ melting was observed (B3H; Table 2). When the crosslinking temperature was increased to 170 °C (C3H), there was no evidence of crystallization (Fig. 5d).

These observations are consistent with the DSC results wherein there was no evidence of crystallization (C3H; Table 2). Thus, thermal crosslinking of the polymer retarded KTZ crystallization and enhanced the physical stability of the system. In addition, the crosslinking temperature provides an avenue to modulate the physical stability at high drug loading.

3.5. Water sorption and onset of crystallization to measure the physical stability of the crosslinked amorphous systems

In the glassy state, crystallization times can be very long due to the low molecular mobility of the system. Water sorption, by plasticizing the system lowers the T_g, enhances molecular mobility leading to drug crystallization [49]. Recently, water sorption was proposed as an

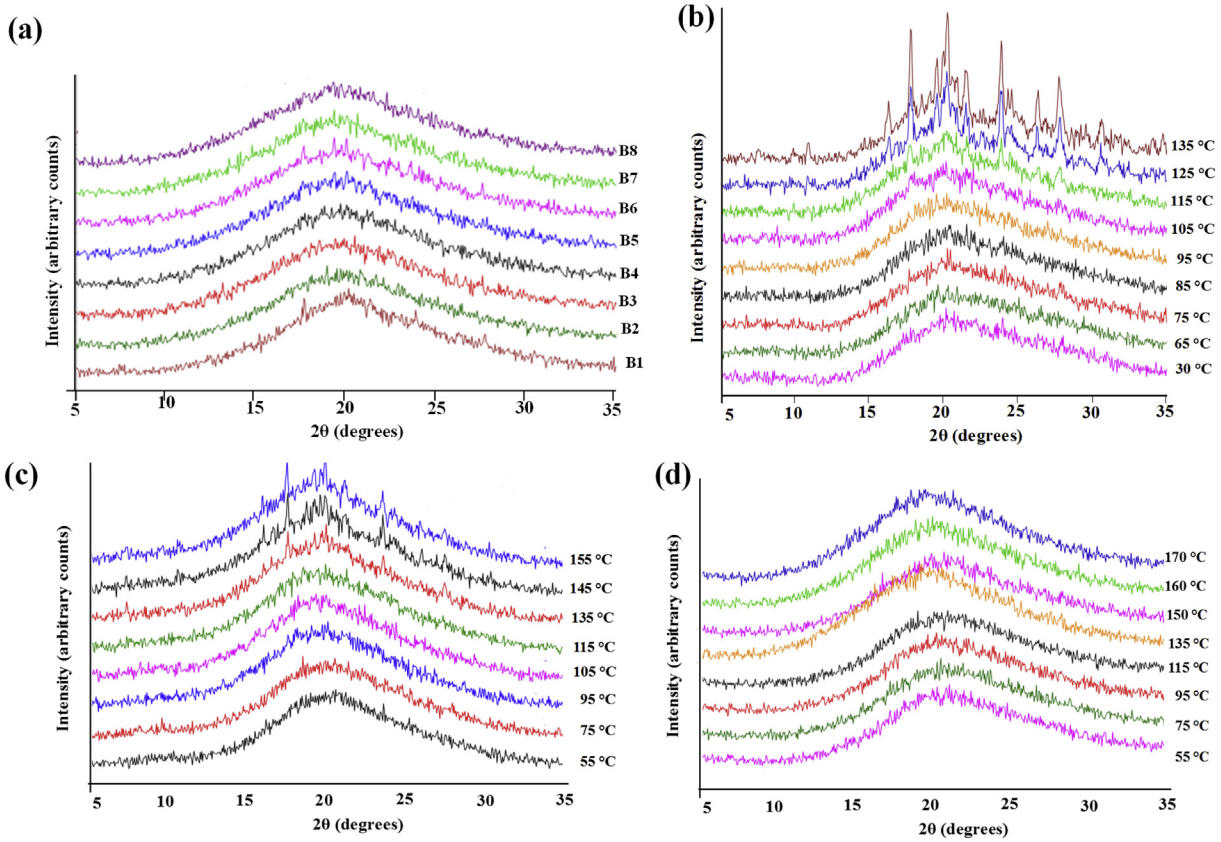

Fig. 5. a) XRD patterns of ASD systems crosslinked at 150 °C for 15 min. The KTZ content was 90% w/w. b–d) Effect of crosslinking temperature on KTZ crystallization condition on first evidence of crystallization. Variable temperature XRD (VTXRD) patterns of crosslinked ASD. b) D2, c) B3H and d) C3H. The temperatures at which the powder patterns were obtained are indicated. KTZ crystallization is evident from the appearance of its characteristic peaks.

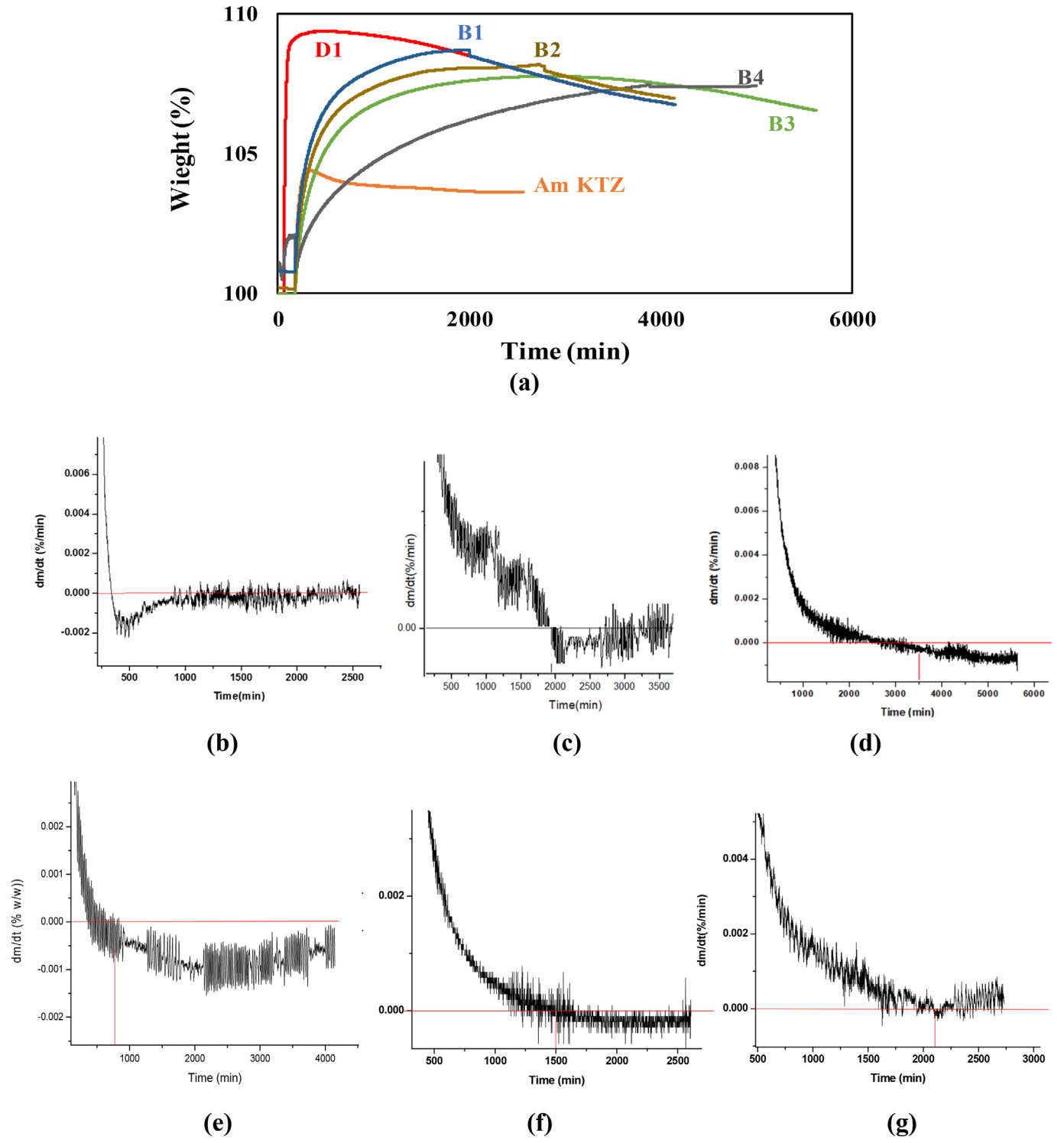

Fig. 6. a) Water sorption behavior of amorphous KTZ, D1 and crosslinked ASDs (B1-B4) following storage at 90% RH/25 °C. The derivative plots of b) amorphous KTZ, c) D1 and (d) B3, clearly reveal the first evidence of weight loss. Water sorption behavior (derivative of curve) of crosslinked ASD with 95% KTZ when stored at 90% RH and 25 °C. e) D2, f) B3H and g) C3H.

accelerated stability testing approach, to predict crystallization times in ASDs [3,4,49].

When exposed to high RH, the initial weight gain is attributable to water sorption. This may be followed by crystallization of plasticized drug, evident from weight loss. Thus, the first evidence of weight loss can be an approximate estimate of the crystallization onset time. Crystallization, accelerated by water vapor sorption, can serve as an effective screening tool to rapidly evaluate and rank order the physical stability of ASDs.

The water sorption profiles of amorphous KTZ following storage at 90% RH/25 °C is shown in Fig. 6a. It initially sorbed water rapidly (~4% w/w), followed by a plateau, and finally began to lose weight at ~250 min. The derivative plot (the change in weight with time, dm/dt) enabled the unambiguous detection of weight loss (negative value of dm/dt; Fig. 6b). With the increase in the crosslinker concentration, there was a progressive decrease in the total amount of sorbed water

(up to 2000 min in Fig. 6a). These are consistent with the results of the swelling study (Fig. 2a). It is interesting that the formation of an ASD by the addition of PAA (10% w/w), resulted in much higher water sorption (compare D1 with amorphous KTZ), and the system resisted crystallization for a much longer time period.

The onset time for crystallization increased as a function of crosslinker concentration as is evident from the derivative plots (Fig. S7; Supplementary Information). The first evidence of weight loss for D1 (control; Fig. 6c), B1, B2 and B3 were observed at 1800, 2200, 2700 and 3500 (Fig. 6d) minutes respectively. In B4, the dispersion with the highest PVA concentration, there was no evidence of crystallization even after 5000 min (Fig. S7; Supplementary Information). Thus, the process of crosslinking stabilized the dispersion (i.e. increase in resistance to crystallization) and this effect was crosslinker concentration dependent. The crosslinking density will increase as a function of crosslinker concentration leading to progressive stability enhancement.

A modest change in the crosslinking condition caused a pronounced change in the crystallization behavior. When the crosslinking temperature was increased from 150 °C (B3; Fig. 6d) to 170 °C (C3), the dispersion resisted crystallization (Fig. S8; Supplementary Information). Finally, the effects of high drug loading (95% w/w) and crosslinking conditions were simultaneously investigated. In the absence of crosslinking, crystallization occurred in ~ 850 min (Fig. 6e). Following crosslinking at 150 °C (B3H), the weight loss was first observed only at ~1500 min (Fig. 6f). However, crystallization was observed only at ~2200 min, when the crosslinking temperature was increased to 170 °C (Fig. 6g).

It is important to recognize that weight loss following water sorption is a consequence of crystallization. However, it is not a direct proof of crystallization. In order to confirm crystallization, the sample was removed after it had sorbed water, crimped hermetically in an aluminum pan and subjected to DSC. KTZ was subjected to DSC after exposure to 90% RH/25 °C for 2500 min. An endotherm was observed at 149.6 °C, with an enthalpy value of 82.9 J/g (Fig. S9; Supplementary Information). This is an excellent agreement with our earlier observations (Fig. 3a) and with literature values [39,40] confirming complete crystallization following water sorption.

However, the DSC results indicated that in crosslinked systems, even after water sorption, there was resistance to crystallization. For example, in B3H, plasticization by the sorbed water was evident from a T_g' observed at 34.0 °C (Fig. S10; Supplementary Information), much lower the T_g of 59 °C of the freshly prepared sample (Table 2). The low enthalpy of crystallization (1.8 J/g), indicated that, following water sorption, crystallization of KTZ was just initiated. In the system crosslinked at 170 °C (C3H) and subjected to water sorption, DSC (Fig. S11; Supplementary Information) did not reveal a melting endotherm suggesting that there was no drug crystallization. This is not surprising, since the water sorption studies (Fig. 6g) did not reveal weight loss after exposure to 90% RH/25 °C for 2500 min.

3.6. Storage stability of the crosslinked ASDs

Elevated temperature and water vapor pressure are known to trigger drug nucleation and accelerate crystallization in solid dispersions. To investigate the physical stability of KTZ ASD, samples prepared under two different crosslinking conditions (95% drug loading) were examined under direct closed vial condition as per the ICH long-term (23 ± 2 °C/32 ± 5% RH) and under open vial conditions for accelerated (40 ± 2 °C/75% ± 5% RH) storage conditions for over 18 months (Table 3). The sample crosslinked at 170 °C/15 min (C3H, Table 2,) resisted crystallization for longer time period than the sample crosslinked at 150 °C/15 min (B3H). This is because of the high crosslinking density of the system, C3H. This robust stability can be predominantly attributed to the ability of the crosslinked matrix to retard KTZ crystallization.

In all cases, > 99.5% of KTZ was retained, reflecting the exceptional stability of the drug underfollowing storage at elevated temperatures and water vapor pressures (Table S1; Supplementary Information.

Table 3
Summary of stability testing of solid dispersions (95% drug loading and crosslinked at 150 °C and 170 °C for 15 min) under ICH long term and accelerated storage conditions after 24 months. The time for which KTZ retained amorphous was given below.

Stability	Storage condition	KTZ retained amorphous for:	
		B3H[a]	C3H[b]
Long term stability	8 ± 3 °C/20 ± 4%RH	> 24 months[c]	> 24 months[c]
	23 ± 3 °C/32 ± 5% RH	> 18 months[c]	> 18 months[c]
Accelerated stability	40 ± 2 °C/75 ± 5% RH	20 days	31 days
	60 ± 2 °C/75 ± 5% RH	4 days	7 days
	80 ± 2 °C/75 ± 5% RH	7 h	17 h
	80 ± 2 °C	2 days	4 days

[a] 95% drug loading; crosslinked at 150 °C/15 min.
[b] 95% drug loading; crosslinked at 170 °C/15 min.
[c] No evidence of crystallization.

3.7. Viscosity of ASDs

The viscosities of the crosslinked amorphous dispersions in the supercooled state were measured over a wide temperature range (Fig. 7). The effects of crosslinker concentration (panel a) and crosslinking temperature (panel b) were investigated. The addition of polymer (10% w/w PAA) to KTZ resulted in an order of magnitude increase in viscosity (D1). This system did not contain any crosslinker. When the crosslinker concentration was progressively increased from 0.25% to 1.0% w/w (the total concentration (polymer + crosslinker) was fixed at 10% w/w), there was approximately four orders of magnitude increase in viscosity.

However, compared to amorphous KTZ, B4 showed a pronounced (over four orders of magnitude) increase in viscosity. As expected from the DES data (Fig. 4a), the temperature dependence of viscosity was non-Arrhenius. Even at a higher drug concentration of 95% w/w, the addition of 5% w/w PAA (no crosslinker) to amorphous KTZ, caused more than half an order of magnitude increase in viscosity. Crosslinking carried out either at 150 °C or at 170 °C, brought about ~ two orders of magnitude increase in viscosity compared to amorphous KTZ. In these systems, the crosslinker concentration was maintained constant (0.75% w/w). At a drug loading of 90% w/w, a similar increase in viscosity was observed when the crosslinking temperature was increased from 150 to 170 °C (B3 and C3 in Fig. 7b).

The viscosity results provide the mechanistic basis for the mobility results presented earlier (Fig. 4a). Thus, an increase, either in crosslinker concentration or reaction temperature, by increasing the crosslink density decreased the viscosity and reduced the molecular mobility. The pronounced resistance to crystallization induced by crosslinking can be attributed to the reduced mobility.

3.8. Dissolution

Fig. 8 shows the dissolution profile of KTZ (amorphous and crystalline) and two crosslinked samples (B3H and C3H; compositions are given in Table 2). Amorphous KTZ crystallized immediately (within 20 min) and the concentration of the drug diminished rapidly and reached a value close to that of the crystalline drug (~589 μg/ml; Fig. 8b). The rapid decrease in concentration revealed the pronounced crystallization tendency of the 'as is' KTZ. This result is consistent with earlier results of rapid recrystallization of felodipine (27). In contrast to amorphous KTZ, the drug dissolution from the crosslinked system is regulated by diffusion where the matrix is insoluble and the dissolved drug (forming a supersaturated solution) diffuses out of the crosslinked network (27). As a result, the degree of supersaturation in the

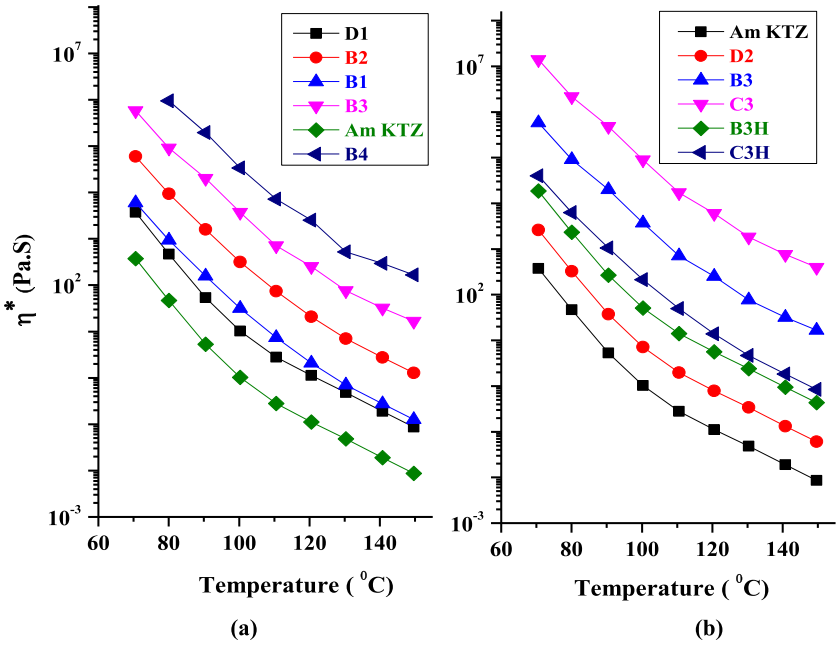

Fig. 7. Plot of viscosity as a function of temperature. a) Effect of crosslinker concentration. b) Effect of crosslinking temperature at drug loading of 90 and 95% w/w (compositions are in Table 1). Y axis is in logarithmic scale. Error bars represent SD and they are smaller than the size of the symbol.

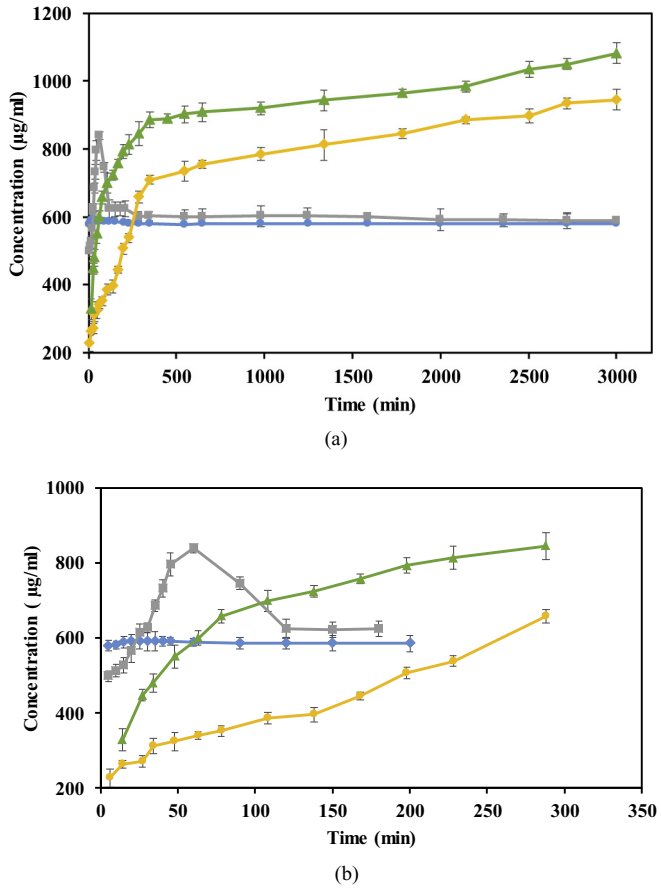

Fig. 8. a) Dissolution profiles of drug (crystalline KTZ and amorphous KTZ) and crosslinked ASDs (mean ± SD; $n = 3$). Green: B3H (95% drug loading and crosslinked at 150 °C/15 min); yellow: C3H (95% drug loading and crosslinked at 170 °C/15 min). The profiles of crystalline (blue) and amorphous (grey) KTZ are also provided. b) The dissolution profiles in the first 300 min. (For interpretation of the references to colour in this figure legend, the reader is referred to the web version of this article.)

dissolution medium generated by the crosslinked system gradually increases (Fig. 8) and is maintained for a prolonged period. The release from B3H results in supersaturation (the concentration of 885 µg /ml at 350 min, is about 1.5 times the equilibrium solubility of crystalline KTZ in the dissolution medium; Fig. 8a). The crosslinked systems, by modulating drug dissolution, avoided the rapid surge in supersaturation and the consequent nucleation and drug crystallization. The crosslinked ASDs exhibited a sustained solubility enhancement, surpassing the amorphous KTZ concentration (27).

The dissolution performance of the different systems can be compared using the area under the curve (AUC) obtained from the concentration-time profiles. In the presence of PAA (i.e. in the ASDs), sustained supersaturation is achieved with B3H exhibiting higher AUC than C3H (Table 4). An increase in crosslinking density (C3H > B3H), decreased the release rate of KTZ (C3H < B3H). With an increase in the degree of cross-linking, the attendant decrease in the degree of swelling slows down the release of the drug from the matrix.

4. Significance

To minimize or eliminate the risk of drug crystallization from ASDs, the current practice in the pharmaceutical community is to prepare dispersions with high polymer concentrations [50,51]. However, for high dose drugs, this can result in an unreasonable “pill burden”. We have demonstrated that crosslinking, by increasing the viscosity and reducing molecular mobility, maintained the drug in amorphous state

Table 4
Dissolution results of KTZ (crystalline and amorphous) and crosslinked ASD systems (B3H and C3H).

Sample ID	AUC(0 → t) (µg/mL min) × 10^6 (mean ± SD)	AUC ratio (mean)
Crystalline KTZ	1.24 ± 0.09	1.00
Amorphous KTZ	1.28 ± 0.16	1.03
B3H	2.09 ± 0.14	1.68
C3H	1.74 ± 0.08	1.40

[a][AUC(0 → t), sample]/[AUC(0 → t), crystalline KTZ].
SD = standard deviation.

even in dispersions with very high drug loading. At 90% w/w drug loading, the physical stability was progressively enhanced by increasing the crosslinker concentration. When the drug loading was raised to 95% w/w, increasing the crosslinking temperature provided a second avenue to enhance physical stability.

Elevation in temperature, specifically $T > T_g$, and plasticization, for example by water sorption, can accelerate drug crystallization from ASDs. When formulated judiciously (for example, C3H in Table 1), the dispersion exhibited exceptional physical stability and resisted crystallization (Fig. 5d; Fig. S8b). We have demonstrated that, the degree of crosslinking, i.e. crosslinking density, provides an avenue to modulate the physical stability of ASDs. This can be accomplished by tuning the crosslinker concentration and the reaction temperature.

The resistance to crystallization increased as a function of crosslinker concentration (Fig. S7: Supplementary Information) as well as crosslinking temperature (Fig. 6). In both instances, an increase in the crosslinking density progressively enhanced stability. However, high crosslinking density can have a potential detrimental effect – the drug release rate can become unacceptably slow. Therefore, the crosslinking density can be tailored so as to obtain the desired release kinetics while the system exhibits adequate physical stability. Again, the most important output from the dissolution study of the crosslinked ASD is that the drug release rate can be modulated so as to attain supersaturation while minimizing the risk of crystallization.

In summary, we have documented that crosslinking, by increasing the viscosity and decreasing molecular mobility, enhanced the physical stability of ASDs. This approach enabled the preparation of stable ASDs with exceptionally high drug loading (up to 95% w/w). Unlike chemical crosslinking, in our approach, the drug loading is not limited by the crosslinking density.

5. Conclusion

Crosslinking, by decreasing molecular mobility, provides an avenue to modulate the physical stability of ASDs either by controlling the crosslinker concentration or crosslinking temperature. With an increase in crosslinker concentration (from 0.25 to 1.0% w/w), there was a progressive reduction in molecular mobility revealed by the increase in viscosity and the longer α-relaxation times. There was an attendant increase in physical stability as evident from the inhibition of KTZ crystallization. The physical stability of the crosslinked system can be further enhanced by raising the crosslinking temperature. This approach resulted in a stable ASD even at a high drug loading (95% w/w drug). Again, during dissolution study, the degree of supersaturation in the dissolution medium generated by the crosslinked systems gradually increased and maintained the supersaturation for a longer period. This approach may result in formulations that exhibited a better biopharmaceutical performance than the amorphous KTZ.

Acknowledgements

This work was partially supported by the William and Mildred Peters endowment fund (1701-11392-20662-UMF0003766-2108004). Parts of this work were carried out in the Characterization Facility, University of Minnesota, a member of the National Science Foundation-funded Materials Research Facilities Network (www.mrfn.org).

Declaration of Competing Interest

The authors declare no competing financial interest.

Appendix A. Supplementary data

Supplementary data to this article can be found online at https://doi.org/10.1016/j.jconrel.2019.09.007.

References

[1] A.T.M. Serajuddin, Solid dispersion of poorly water-soluble drugs: early promises, subsequent problems, and recent breakthroughs, J. Pharm. Sci. 88 (1999) 1058.
[2] T. Vasconcelos, B. Sarmento, P. Costa, Solid dispersions as strategy to improve oral bioavailability of poor water-soluble drugs, Drug Discov. Today 12 (2007) 1068.
[3] S. Baghel, H. Cathcart, N.J. O'Reilly, Polymeric amorphous solid dispersions: a review of amorphization, crystallization, stabilization, solid-state characterization, and aqueous solubilization of biopharmaceutical classification system class II drugs, J.Pharm.Sci. 105 (2016) 2527.
[4] B.V. Slaughter, S.S. Khurshid, O.Z. Fisher, A. Khademhosseini, N.A. Peppas, Hydrogels in regenerative medicine, Adv. Mater. 21 (2009) 3307.
[5] G. Giammona, G. Pitarresi, V. Tomarchio, G. Cavallaro, M. Mineo, Crosslinked α,β-poly asparthydrazide hydrogels: effect of crosslinking degree and loading method on cytarabine release rate, J. Control. Release 41 (1996) 195.
[6] T. Miyata, T. Uragami, K. Nakamae, Biomolecule-sensitive hydrogels, Adv. Drug Deliv. Rev. 54 (2002) 79.
[7] F. Yokoyama, I. Masada, K. Shimamura, T. Ikawa, K. Monobe, Morphology and structure of highly elastic poly (vinyl alcohol) hydrogel prepared by repeated freezing-and-melting, Colloid Polym. Sci. 264 (1986) 595.
[8] W. Teng, J. Capello, X. Wu, Physical crosslinking modulates sustained drug release from recombinant silk-elastin like protein polymer for ophthalmic applications, J. Control. Release 156 (2011) 186.
[9] L. Stringer, N.A. Peppas, Diffusion of small molecular weight drugs in radiation-crosslinked poly (ethylene oxide) hydrogels, J. Control. Release 42 (1996) 195.
[10] R. Tandon, P. Attri, R. Bhatia, Chemical crosslinking: role in protein and peptide science, Curr. Protein Pept. Sci. 18 (2017) 946.
[11] M. Tsukasa, T. Yuuki, A. Sachiko, I. Takahiko, H. Akie, E. Keiko, Role of boric acid for a poly (vinyl alcohol) film as crosslinking agent: melting behavior of this films with boric acid, Polymer 51 (2010) 5539.
[12] J. Maitra, V.K. Shukla, Cross-linking in hydrogels - a review, Am. J. Polym. Sci. 4 (2014) 25.
[13] K.T. Nguyen, J.L. West, Photopolymerizable hydrogel for tissue engineering applications, Biomaterials 23 (2002) 4307.
[14] N.A. Peppas, P. Bures, W. Leobandung, H. Ichikawa, Hydrogels in pharmaceutical formulations, Eur. J. Pharm. Biopharm. 50 (2000) 27.
[15] A.S. Sawhney, C.P. Pathak, J.J. van Rensburg, R.C. Dunn, J.A. Hubbell, Optimization of photo polymerized biodegradable hydrogel properties for adhesion prevention, J. Biomed. Mater. Res. 28 (1994) 831.
[16] J. Kopecek, Hydrogel biomaterials: a smart future? Biomaterials 28 (2007) 5185.
[17] M.P. Lutolf, Biomaterials: spotlight on hydrogels, Nat. Matter. 8 (2009) 451.
[18] L. Carpentier, M. Bourgeois, Contribution of temperature modulated DSC to the study of the molecular mobility in glass forming pharmaceutical systems, J. Therm. Anal. Calorim. 68 (2002) 727.
[19] K. Kuwabara, Z. Gan, T. Nakamura, H. Abe, Y. Doi, Molecular mobility and phase structure of biodegradable poly (butylene succinate) and poly (butylene succinate-co-butylene adipate), Biomacromolecules 3 (2002) 1095.
[20] F. Román, P. Colomer, Y. Calventus, J.M. Hutchinson, Molecular mobility in hyper branched polymers and their interaction with an epoxy matrix, Materials 9 (2016) 192.
[21] R. Yang, R. Wei, K. Li, L. Tong, K. Jia, X. Liu, Crosslinked polyarylene ether nitrile film as flexible dielectric materials with ultrahigh thermal stability, Sci. Rep. 6 (2016) 36434.
[22] Y. Aras, B.M. Baysal, Dielectric relaxation studies of some linear crosslinked and branched polymers, J. Polym. Sci. Polym. Phys. 22 (1984) 1453.
[23] V.Y. Kramarenko, T.A. Ezquerra, I. Šics, F.J. Baltá-Calleja, V.P. Privalko, Influence of cross-linking on the segmental dynamics in model polymer networks, J. Chem. Phys. 113 (1) (2000) 447.
[24] S. Oprea, V.E. Musteata, V.O. Potolinca, Molecular dynamics of linear and cross-linked polyester urethanes studied by dielectric spectroscopy, J. Elastomers Plast. 43 (2011) 559.
[25] T. Nicolai, Dielectric relaxation of linear and cross-linked polyurethane, Macromolecules 34 (2001) 8995.
[26] L. Okrasa, P. Czech, G. Boiteux, F. Méchin, J. Ulanskia, Molecular dynamics in polyester- or polyether-urethane networks based on different diisocyanates, Polymer 49 (2008) 2662.
[27] P. Zahedi, P.I. Lee, Solid molecular dispersions of poorly water-soluble drugs in poly (2-hydroxyethyl methacrylate) hydrogels, Eur. J. Pharm. Biopharm. 65 (2007) 320.
[28] D.D. Sun, T.C. RobJu, P.I. Lee, Enhanced kinetic solubility profiles of indomethacin amorphous solid dispersions in poly(2-hydroxymethacrylate) hydrogels, Eur. J. Pharm. Biopharm. 81 (2012) 149.
[29] P. Mistry, R. Suryanarayanan, Strength of drug- polymer interaction: an implication for crystallization in dispersions, Cryst. Growth Des. 16 (2016) 5141.
[30] M.H. Fung, M. DeVault, K.T. Kuwata, R. Suryanarayanan, Physical stability and dissolution behavior of ketoconazole–organic acid coamorphous systems, Mol. Pharm. 15 (2018) 1052.
[31] J.W. Lubach, J.Z. Chen, J. Hau, J. Imperio, M. Coraggio, L. Liu, H. Wong, Investigation of the rat model for preclinical evaluation of pH-dependent oral absorption in humans, Mol. Pharm. 10 (2013) 3997.
[32] P. Kanaujia, G. Lau, W.K. Nag, E. Widjaja, A. Hanefeld, M. Fischbach, M. Maio, R.B. Tan, Nanoparticle formation and growth during in vitro dissolution of ketoconazole solid dispersion, J. Pharm. Sci. 100 (2011) 2876.
[33] C. Bhugra, R. Shmeis, S.L. Krill, M.J. Pikal, Prediction of onset of crystallization from experimental relaxation times I- correlation of molecular mobility from temperatures above the glass transition to temperatures below the glass transition,

Pharm. Res. 23 (2006) 2277.
[34] F.A. Martin, M.M. Pop, G. Borodi, X. Filip, I. Kacso, Ketoconazole salt and co-crystals with enhanced aqueous solubility, Cryst. Growth Des. 13 (2013) 4295.
[35] K. Kumeta, I. Nagashima, S. Matsui, K. Mizoguchi1, Crosslinking reaction of poly (vinyl alcohol) with poly (acrylic acid) (PAA) by heat treatment: effect of neutralization of PAA, J. Appl. Polym. Sci. 90 (2003) 2420.
[36] M.C. Koetting, J.F. Guido, M. Gupta, A. Zhang, N.A. Peppas, pH-responsive and enzymatically-responsive hydrogel microparticles for the oral delivery of therapeutic proteins: effects of protein size, crosslinking density, and hydrogel degradation on protein delivery, J. Control. Release 221 (2016) 18.
[37] P.G. Shukla, N. Rajagopalan, C. Bhaskar, S. Sivaram, Crosslinked starch-urea formaldehyde (St-UF) as a hydrophilic matrix for encapsulation: studies in swelling and release of carbofuran, J. Control. Release 15 (1991) 153.
[38] G. Van den Mooter, M. Wuyts, N. Blaton, R. Busson, P. Grobet, P. Augustijns, R. Kinget, Physical stabilization of amorphous ketoconazole in solid dispersions with polyvinylpyrrolidone K25, Eur. J. Pharm. Sci. 12 (2001) 261.
[39] A.C. Rumondor, I. Ivanisevic, S. Bates, D.E. Alonzo, L.S. Taylor, Evaluation of drug-polymer miscibility in amorphous solid dispersion systems, Pharm. Res. 26 (2009) 2523.
[40] G. Fox, S. Loshaek, Influence of molecular weight and degree of crosslinking on the specific volume and glass temperature of polymers, J. Polym. Sci. 15 (1955) 371.
[41] S. Bhattacharya, R. Suryanarayana, Local mobility in amorphous pharmaceuticals—characterization and implications on stability, J. Pharm. Sci. 98 (2009) 2935.
[42] R. Richert, F. Stickel, R.S. Fee, M. Maroncelli, Solvation dynamics and the dielectric response in a glass-forming solvent: from picoseconds to seconds, Chem. Phys. Lett. 229 (1994) 302.
[43] P. Mistry, S. Mohapatra, T. Gopinath, F.G. Vogt, R. Suryanarayanan, Role of strength of drug-polymer interactions on the molecular mobility and crystallization inhibition in ketoconazole solid dispersions, Mol. Pharm. 12 (2015) 3339.
[44] G. Williams, D.C. Watts, Non-symmetrical dielectric relaxation behavior arising from a simple empirical decay function, Trans. Faraday Soc. 66 (1970) 80.
[45] F. Alvarez, A. Alegria, J. Colmenero, Relationship between the time-domain Kohlrausch-Williams-Watts and frequency-domain Havriliak-Negami relaxation functions, Phys. Rev. B 44 (1991) 7306.
[46] S.P. Bharadwaj, K.K. Arora, E. Kwong, A. Templeton, S. Dorothee Clas, R. Suryanarayanan, Mechanism of amorphous itraconazole stabilization in polymer solid dispersions: role of molecular mobility, Mol. Pharm. 10 (2013) 694.
[47] S.L. Shamblin, B.C. Hanckck, Y. Dupuis, M.J. Pikal, Interpretation of relaxation time constants for amorphous pharmaceutical systems, J. Pharm. Sci. 89 (2000) 417.
[48] E. Tombari, C. Ferrari, G.P. Johari, R.M. Shanker, Calorimetric relaxation in pharmaceutical molecular glasses and its utility in understanding their stability against crystallization, J. Phys. Chem. B 112 (2008) 10806.
[49] S. Greco, J. Authelin, C. Leveder, A. Segalini, A practical method to predict physical stability of amorphous solid dispersions, Pharm. Res. 29 (2012) 2792.
[50] J.S. Kim, S.J. Lee, H.C. Chang, M.S. Lee, Pharmaceutical Solid Dispersions Comprising Ubidecarenone. *WO2007086689A1*, (2007).
[51] F. Theil, S. Anantharaman, S.O. Kyerematen, H. Lishaut, S.H. Dreis-Kühne, J. Rosenberg, M. Mägerlein, G.H. Woehrle, Frozen in time: kinetically stabilized amorphous solid dispersions of nifedipine stable after a quarter century of storage, Mol. Pharm. 14 (2017) 183.